Nanoparticle Delivery of Proangiogenic Transcription Factors into the Neonatal Circulation Inhibits Alveolar Simplification Caused by Hyperoxia

Craig Bolte[1,3], Vladimir Ustiyan[1,3], Xiaomeng Ren[1,3], Andrew W. Dunn[1,3,5], Arun Pradhan[1,3], Guolun Wang[1,3], Olena A. Kolesnichenko[1,3], Zicheng Deng[1,3,5], Yufang Zhang[1,3], Donglu Shi[5], James M. Greenberg[1,2], Alan H. Jobe[1,2], Tanya V. Kalin[1,2] and Vladimir V. Kalinichenko[1,2,3,4]*

[1]Department of Pediatrics, University of Cincinnati and Cincinnati Children's Hospital Medical Center, 3333 Burnet Avenue, Cincinnati, OH 45229; [2]Division of Pulmonary Biology, Cincinnati Children's Hospital Medical Center, 3333 Burnet Avenue, Cincinnati, OH 45229; [3]Center for Lung Regenerative Medicine, Cincinnati Children's Hospital Medical Center, 3333 Burnet Avenue, Cincinnati, OH 45229; [4]Division of Developmental Biology, Cincinnati Children's Hospital Medical Center, 3333 Burnet Avenue, Cincinnati, OH 45229; [5]The Materials Science and Engineering Program, College of Engineering and Applied Science, University of Cincinnati, Cincinnati, OH 45221.

Online Supplementary Materials

SUPPLEMENTAL FIGURE LEGENDS

Supplemental Figure E1. Hydrodynamic diameter, zeta potential and DNA binding capacity of PEI_{600}-MA_5/PEG-OA/Cho nanoparticles. ***(A)*** Gel electrophoresis shows the binding of synthesized PEI_{600}-MA_5 to plasmid DNA. Numbers above lanes refer to the mass ratio (w/w) of polymer:plasmid. Full restriction is observed at a w/w of 6. ***(B)*** ^1H NMR ($CDCl_3$, 400 MHz) of polyethylenimine Mn = 600 (PEI_{600}), myristic acid (MA), and conjugated PEI_{600}-MA_5.Conjugation shifts α-carbon (i) resonance upfield (2.35 -> 2.17) while broadening PEI resonance. ***(C)*** Hydrodynamic diameter of PEI_{600}-MA_5/PEG-OA/Cho nanoparticles mixed with DNA (w/w = 24, 153 ± 68 nm) and without DNA (w/w = 0, 325 ± 308 nm). ***(D)*** Zeta potential (charge) of PEI_{600}-MA_5/PEG-OA/Cho nanoparticles mixed with DNA (w/w = 24) is +18.3 ± 5.2 mV. Zeta potential of the nanoparticles without DNA (w/w = 0) is +34.9 ± 9.6 mV.

Supplemental Figure E2. Nanoparticle delivery of *CMV-empty* plasmid does not change alveolar simplification caused by neonatal hyperoxia. H&E staining of lung paraffin sections shows alveolar simplification in mice treated with hyperoxia (HO) alone and HO with nanoparticle delivery of *CMV-empty* plasmid. Mice were exposed to HO or room air (RA) from P1 to P7 followed by RA exposure until lung harvest at P28. Nanoparticle delivery was performed at P2. Nanoparticle delivery of *CMV-empty* plasmid does not improve lung structure in hyperoxia-treated mice. Magnification: top panels, x200; bottom panels, x400.

Supplemental Figure E3. PEI_{600}-MA_5/PEG-OA/Cho nanoparticles deliver *CMV-GFP* into pulmonary microvascular endothelial cells. ***(A)*** Confocal images show that GFP is present in perinuclear regions of endothelial cells stained with PECAM-1 (arrowheads). *CMV-GFP* plasmid was incapsulated into nanoparticles and the nanoparticle DNA complexes were injected at P2.

Lungs were harvested at P5. Controls include delivery of nanoparticles containing *CMV-empty* plasmid. Scale bars are 10μm (top panels) and 2μm (bottom panels). ***(B)*** High magnification confocal images show the presence of GFP (green) and DyLight 650 quantum dots (purple) in microvascular lung EC stained with PECAM-1. Cell nuclei were stained with DAPI (blue). Cell surface PECAM-1 was removed using a deconvolution option in Imaris software (bottom image), indicating the presence of GFP and DyLight 650 inside the cell. Scale bars are 2μm.

Supplemental Figure E4. PEI_{600}-MA_5/PEG-OA/Cho nanoparticles deliver *CMV-Foxf1* plasmid to pulmonary endothelial cells and myofibroblasts. ***(A)*** *CMV-Foxf1* plasmid was incapsulated into nanoparticles and nanoparticle DNA complexes were injected at P2. Lungs were harvested at P4. FACS sorting was used to purify endothelial cells ($CD31^+CD45^-CD326^-$, abbreviated CD31) and myofibroblasts ($CD140a^+CD31^-CD45^-CD326^-$, abbreviated CD140a). Nanoparticles with CMV-empty plasmid were used as a control (CMV). RNA was prepared from FACS-sorted cells. After DNAse treatment and the reverse transcriptase step, three different concentrations of cDNA (1x, 2x and 3x) were analyzed. RT-PCR shows the presence of exogenous, plasmid-derived *Foxf1* mRNA in endothelial cells and myofibroblasts. Expression levels of exogenous *Foxf1* mRNA were higher in endothelial cells compared to myofibroblasts (n=3-4 mice per group), $p<0.05$ is *, $p<0.01$ is **. ***(B)*** Schematic shows *CMV-Foxf1* expression plasmid, which was incapsulated into nanoparticles. Forward primer (HA) and reverse primer (F1-Rev) were used to amplify the 595bp PCR product. ***(C)*** Exogenous *Foxf1* mRNA was undetectable in FACS-sorted cells at P12.

Supplemental Figure E5. PEI_{600}-MA_5/PEG-OA/Cho nanoparticles target microvascular endothelial cells but not endothelial cells of large blood vessels. Confocal images show that GFP (green) is present in perinuclear regions of endothelial cells (arrowheads) stained with

endomucin (red). Cell nuclei were stained with DAPI (blue). *CMV-GFP* plasmid was incapsulated into nanoparticles and the polymer/ DNA complexes were injected at P2. Lungs were harvested at P5. Controls include delivery of nanoparticles containing *CMV-empty* plasmid. Abbreviations: EC, endothelial cell; al, alveolus; V, blood vessel. Scale bars are 10μm (top panels) and 2μm (bottom panels).

Supplemental Figure E6. Intratracheal delivery of PEI_{600}-MA_5/PEG-OA/Cho nanoparticles is ineffective for targeting of pulmonary cell types. Fluorescently-labeled (DyLight 650) nanoparticles were used for intratracheal delivery in P2 mice. Lungs were harvested at P5 and used for FACS analysis. FACS gating strategy and fluorescence profiles are shown for hematopoietic (a), endothelial (b), epithelial (c) and stromal cells (d). DyLight 650 is shown by colored lines in individual mice (n=4). PEI_{600}-MA_5/PEG-OA/Cho nanoparticles do not target pulmonary cell types after intratracheal delivery.

Supplemental Figure E7. Nanoparticle delivery of FOXM1 or FOXF1 increases capillary density in hyperoxia-treated lungs. ***(A)*** Endomucin staining and confocal imaging show alveolar microvascular networks (green) in alveolar regions of P28 mice. Mice were exposed to hyperoxia (HO) or room air (RA) from P1 to P7 followed by RA exposure until the lung harvest at P28. PEI_{600}-MA_5/PEG-OA/Cho nanoparticles containing *CMV-Foxm1*, *CMV-Foxf1* or *CMV-empty* (control) were delivered at P2 via the facial vein. DAPI was used to stain cell nuclei. Capillary density in HO-treated lungs is increased after nanoparticle delivery of FOXM1 or FOXF1. ***(B)*** Intravascular labeling with Isolectin B4 (green) shows that nanoparticle delivery of *CMV-Foxm1* or *CMV-Foxf1* increases capillary density in alveolar regions. Isolectin B4 was i. v. injected 1hr before harvesting the mice at P14. Scale bars are 30μm.

Supplemental Figure E8. Nanoparticle delivery of FOXM1 or FOXF1 improves endothelial coverage in alveoli of hyperoxia-treated mice. Immunostaining for PECAM-1 (dark purple) shows alveolar microvascular networks in P28 lungs. Mice were exposed to hyperoxia or room air (RA) from P1 to P7 followed by RA exposure until lung harvest at P28. Nanoparticles containing *CMV-Foxm1*, *CMV-Foxf1* or *CMV-empty* (control) were delivered at P2. Nuclear fast red (red) was used for counterstaining. Endothelial coverage in alveoli (arrowheads) is improved after nanoparticle delivery of FOXM1 or FOXF1. Arrows show the absence of PECAM-1 staining in alveolar septa. Scale bars are 50μm.

Supplemental Figure E9. Increasing the dose of *CMV-Foxm1*/ nanoparticle complexes does not improve biological effects. ***(A-B)*** H&E staining (A) and immunostaining for endomucin (B) show alveolar structure and capillary density in P28 lungs. Mice were exposed to hyperoxia (HO) or room air (RA) from P1 to P7 followed by RA exposure until lung harvest at P28. Two different doses of nanoparticles containing either *CMV-Foxm1* or *CMV-empty* (CMV) (5μg and 10μg) were delivered at P2. ***(C-D)*** Both concentrations of nanoparticle/ *CMV-Foxm1* complexes decrease alveolar size (C) and increase capillary density (D). The percentage of airspaces was calculated using 10 random H&E-stained lung images. Endomucin-stained area was quantified using 10 random lung images (n=3 mice), $p<0.01$ is **, $p<0.05$ is *, n.s. is not significant.

Supplemental Figure E10. Delivery of either *CMV-Foxm1* or *CMV-Foxf1* plasmids without nanoparticles does not affect alveolarization and angiogenesis after neonatal hyperoxic injury. ***(A-B)*** H&E staining (A) and immunostaining for endomucin (B) show alveolar structure and capillary density in P28 lungs. Mice were exposed to hyperoxia (HO) or room air (RA) from P1 to P7 followed by RA exposure until lung harvest at P28. *CMV-Foxm1, CMV-Foxf1* or *CMV-empty* (CMV) plasmids without nanoparticles were i. v. injected at P2. ***(C-D)*** Delivery of plasmid

DNAs without nanoparticles does not affect alveolar size (C) and capillary density (D). The percentage of airspaces was calculated using 10 random H&E-stained lung images. Endomucin-stained area was quantified using 10 random lung images (n=3 mice), $p<0.01$ is **, n.s. is not significant.

Supplemental Figure E11. Nanoparticle delivery of FOXM1 or FOXF1 decreases arterial remodeling in hyperoxia-treated lungs. ***(A-B)*** Mice were exposed to hyperoxia (HO) or room air (RA) from P1 to P7 followed by RA exposure until lung harvest at P28. Nanoparticles containing *CMV-Foxm1*, *CMV-Foxf1* or *CMV-empty* (control) were delivered at P2. Pulmonary arteries are shown with green arrowheads (A). H&E staining shows that hyperoxia exposure causes lung remodeling and thickening of arterial walls (B). Nanoparticle delivery of FOXM1 or FOXF1 decreases arterial remodeling after hyperoxia. ***(C)*** H&E staining shows the location and structure of pulmonary arteries and veins in room air-exposed mice. ***(D-E)*** Immunostaining for αSMA (red) and endothelial markers PECAM-1 and Endomucin (green) was performed using room air-exposed lungs and shows smooth muscle layers in pulmonary arteries and veins. Abbreviations: Ar, artery; V, vein; Br, bronchiole. Magnification: top panels, x100; bottom panels, x400.

Supplemental Figure E12. Delivery of either *CMV-Foxm1* or *CMV-Foxf1* plasmids to room air-exposed mice does not affect alveolarization and angiogenesis without injury. ***(A-B)*** H&E staining (A) and immunostaining for endomucin (B) show alveolar structure and capillary density in P28 lungs. Mice were exposed to room air (RA) from P1 until lung harvest at P28. Nanoparticles with *CMV-Foxm1, CMV-Foxf1* or *CMV-empty* (CMV) plasmids were i. v. injected at P2. ***(C-D)*** Delivery of plasmid DNAs does not affect alveolar sizes (C) and capillary density (D) without lung injury. The percentage of airspaces was calculated using 10 random H&E-stained lung

images. Endomucin-stained area was quantified using 10 random lung images (n=3 mice), n.s. is not significant.

Supplemental Figure E13. Nanoparticle delivery of FOXM1 or FOXF1 does not prevent the loss of pulmonary endothelial cells or alter body weight after hyperoxic injury. ***(A)*** Bar graph shows body weights of P7 mice at the end of neonatal hyperoxia exposure. Mice were exposed to hyperoxia (HO) or room air (RA) from P1 to P7. Nanoparticles containing *CMV-Foxm1, CMV-Foxf1* or *CMV-empty* (CMV) plasmids were i. v. injected at P2. Mice were harvested at P7. HO decreases body weights in neonatal mice (n=4-6 mice per group). ***(B)*** H&E staining shows alveolar simplification in all hyperoxia-treated groups at the end of lung injury. Representative images are shown from n=3 mice in each group. ***(C)*** FACS analysis shows that HO decreases total numbers endothelial cells in lung tissue (n=3 mice). FACS was performed at P7. Endothelial cells were identified as $CD31^{+}CD45^{-}$ live cells. ***(D)*** Nanoparticles containing *CMV-Foxm1*, *CMV-Foxf1* or *CMV-empty* (CMV) equally targeted pulmonary endothelial cells at P7 (n=3 mice per group), $p<0.01$ is **. NS is non-significant differences.

Supplemental Figure E14. Nanoparticle delivery of FOXM1 or FOXF1 does not change endothelial cell viability after hyperoxic injury. ***(A)*** FACS gaiting strategy to identify endothelial cells (EC, $CD31^{+}CD45^{-}$) in lung tissue. Mice were exposed to hyperoxia (HO) or room air (RA) from P1 to P7. FACS analysis of enzymatically-digested lung tissue was performed at the end of hyperoxia injury at P7. Nanoparticles containing *CMV-Foxm1*, *CMV-Foxf1* or *CMV-empty* (control) were delivered at P2. 7-AAD viability dye was used to identify necrotic ECs. Dot plots show FACS analysis of cells obtained from HO-treated lungs. ***(B)*** Percentages of necrotic ECs were quantified (n=3-4 mice per group) and show no changes after nanoparticle delivery of FOXM1 or FOXF1. ***(C)*** Bar graph shows a comparison between ECs with nanoparticles and ECs

without nanoparticles. Cell viability is similar in ECs containing nanoparticle-DNA complexes (Nanoparticle^{+} EC) compared to ECs without nanoparticles (Nanoparticle^{-} EC) (n=3-4 mice per group). NS is non-significant differences.

Supplemental Figure E15. Nanoparticle/ DNA complexes increase *Flk1* and *Vegfa* mRNAs at the end of lung injury. Mice were exposed to hyperoxia (HO) or room air (RA) from P1 to P7. Nanoparticles containing *CMV-Foxm1*, *CMV-Foxf1* or *CMV-empty* (CMV) were delivered at P2. Mice were harvested at P7. qRT-PCR shows that nanoparticle delivery of DNA plasmids increases *Flk1* and *Vegfa* mRNAs in whole lung RNA (n=3 mice per group). *Flk1* and *Vegfa* mRNA were normalized to *β-actin* mRNA, $p<0.01$ is **. NS is non-significant differences.

Supplemental Figure E16. Nanoparticle delivery of *CMV-Foxm1* or *CMV-Foxf1* increases the number of Ki-67-positive endothelial cells at P9. ***(A)*** Co-localization of Ki-67 (red) with endothelial nuclear marker ERG (green) shows proliferative endothelial cells (yellow, arrows). Mice were exposed to hyperoxia (HO) or room air (RA) from P1 to P7 followed by RA exposure until lung harvest at P9. Nanoparticles containing either *CMV-Foxm1, CMV-Foxf1* or *CMV-empty* (CMV) were delivered at P2. ***(B)*** Co-localization of Ki-67 with macrophage marker MAC3 shows proliferative macrophages (arrowheads). Inserts show high magnification images of Ki-67-positive macrophages. ***(C-D)*** Nanoparticle delivery of *CMV-Foxm1* or *CMV-Foxf1* increases the proliferation of endothelial cells (C) but does not change the proliferation of macrophages at P9 (D). Percentages of Ki-67-positive endothelial cells and macrophages were calculated using 10 random images (n=3 mice), $p<0.01$ is **, $p<0.05$ is *, n.s. is not significant.

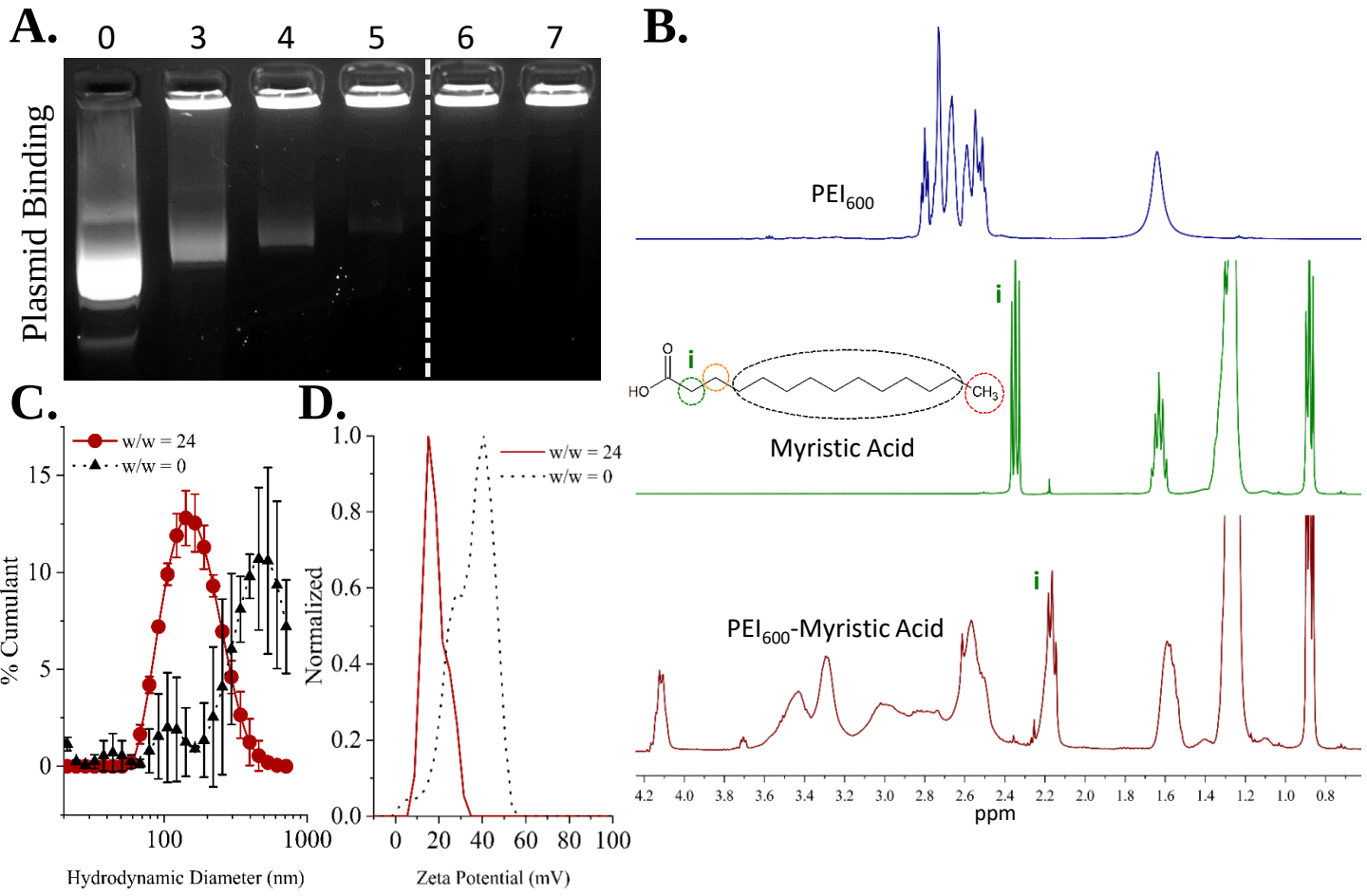
A.
0
3
4
5
6
7
Plasmid Binding
B.
PEI600
i
HO
O
CH3
Myristic Acid
PEI600-Myristic Acid
4.2 4.0 3.8 3.6 3.4 3.2 3.0 2.8 2.6 2.4 2.2 2.0 1.8 1.6 1.4 1.2 1.0 0.8
ppm
C.
w/w = 24
w/w = 0
% Cumulant
15
10
5
0
100
1000
Hydrodynamic Diameter (nm)
D.
w/w = 24
w/w = 0
Normalized
1.0
0.8
0.6
0.4
0.2
0.0
0 20 40 60 80 100
Zeta Potential (mV)

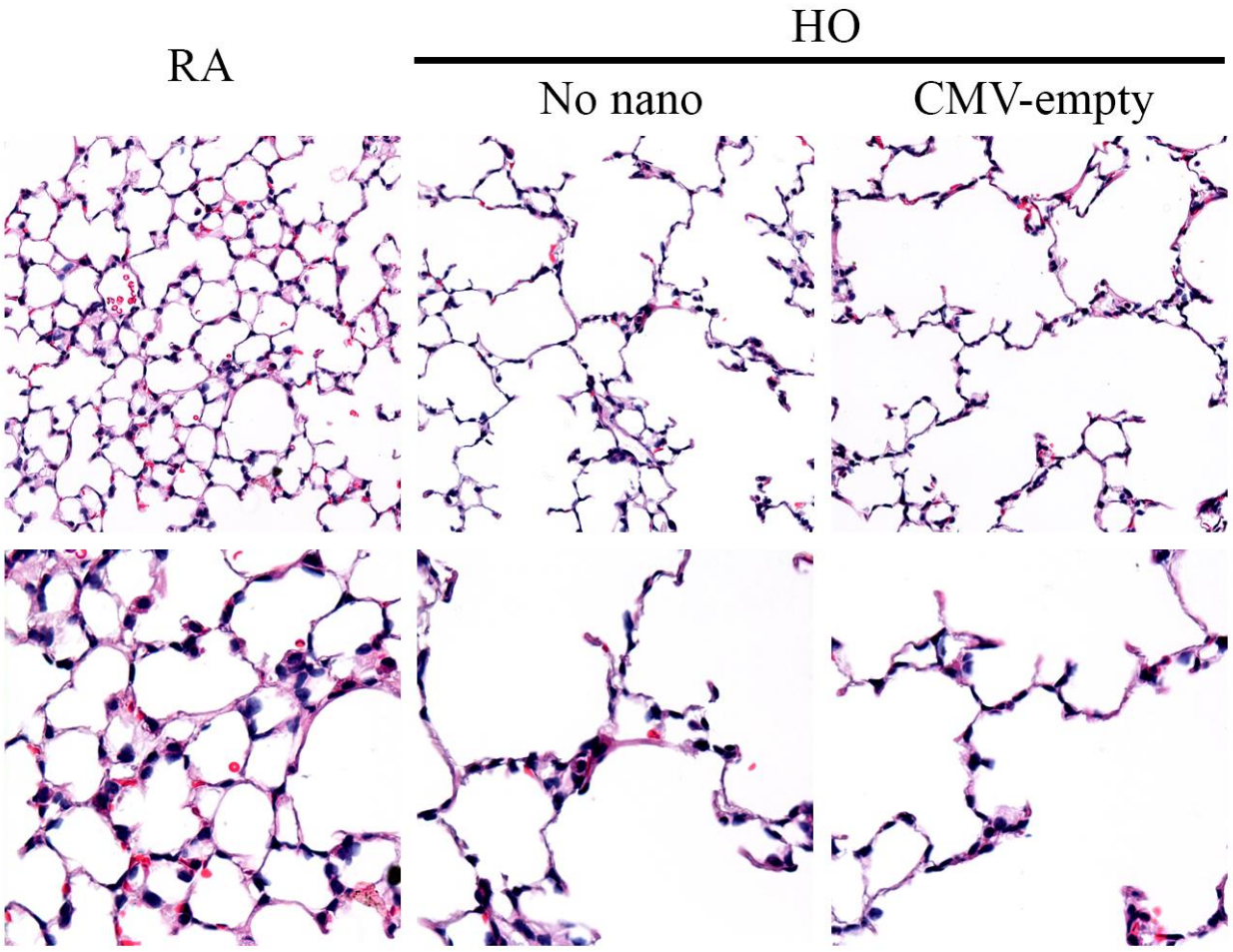
RA
HO
No nano
CMV-empty

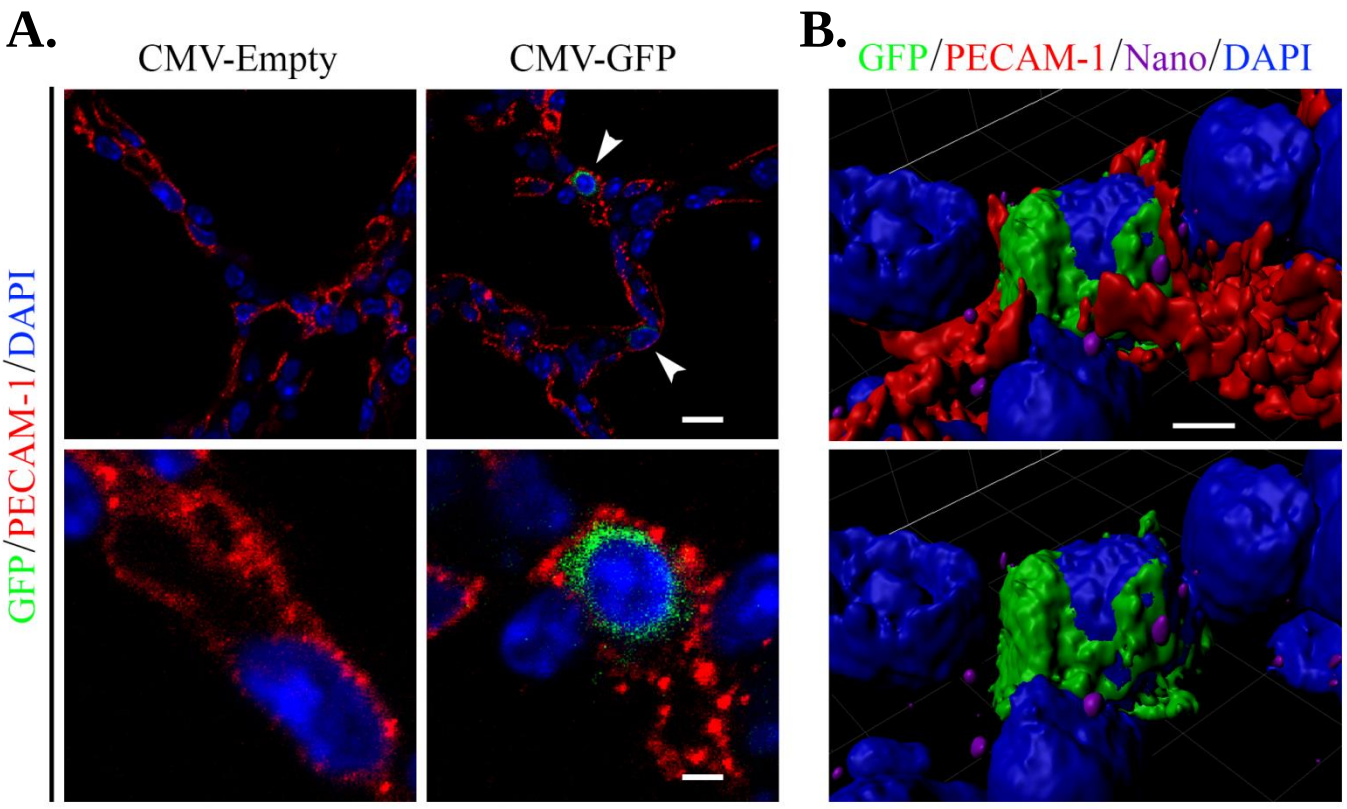
A.
CMV-Empty
CMV-GFP
GFP/PECAM-1/DAPI
B.
GFP/PECAM-1/Nano/DAPI

A.

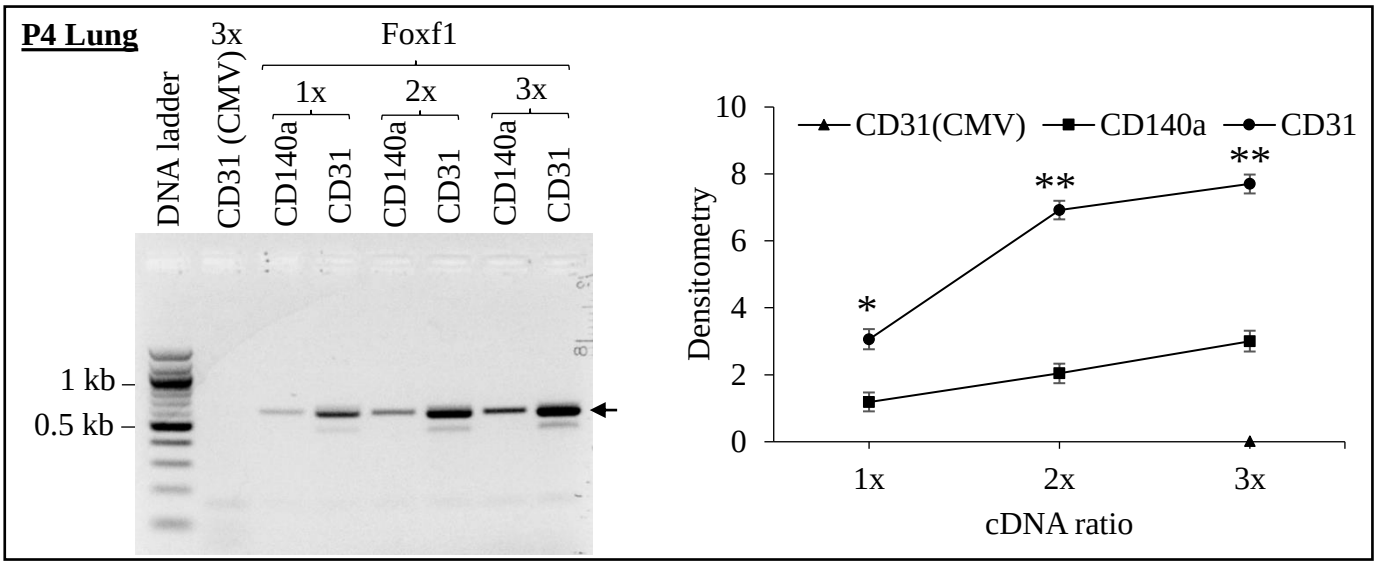
P4 Lung
DNA ladder
CD31 (CMV)
3x
Foxf1
1x
2x
3x
CD140a
CD31
1 kb
0.5 kb
Densitometry
CD31(CMV)
CD140a
CD31
cDNA ratio
1x
2x
3x
*
**
**

B.

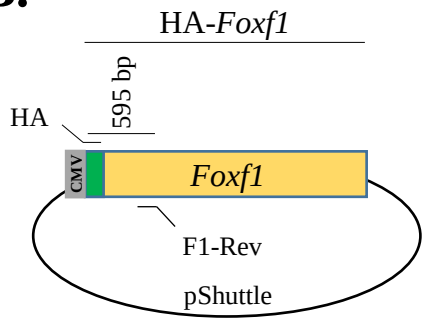
HA-Foxf1
HA
595 bp
CMV
Foxf1
F1-Rev
pShuttle

C.

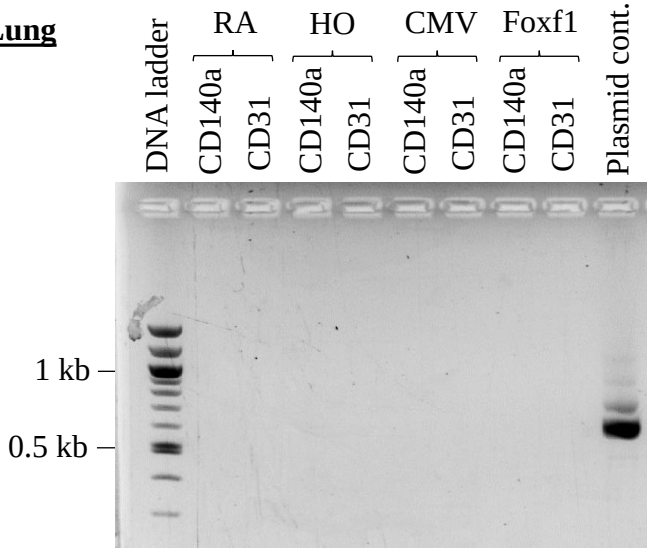
P12 Lung
DNA ladder
RA
HO
CMV
Foxf1
CD140a
CD31
Plasmid cont.
1 kb
0.5 kb

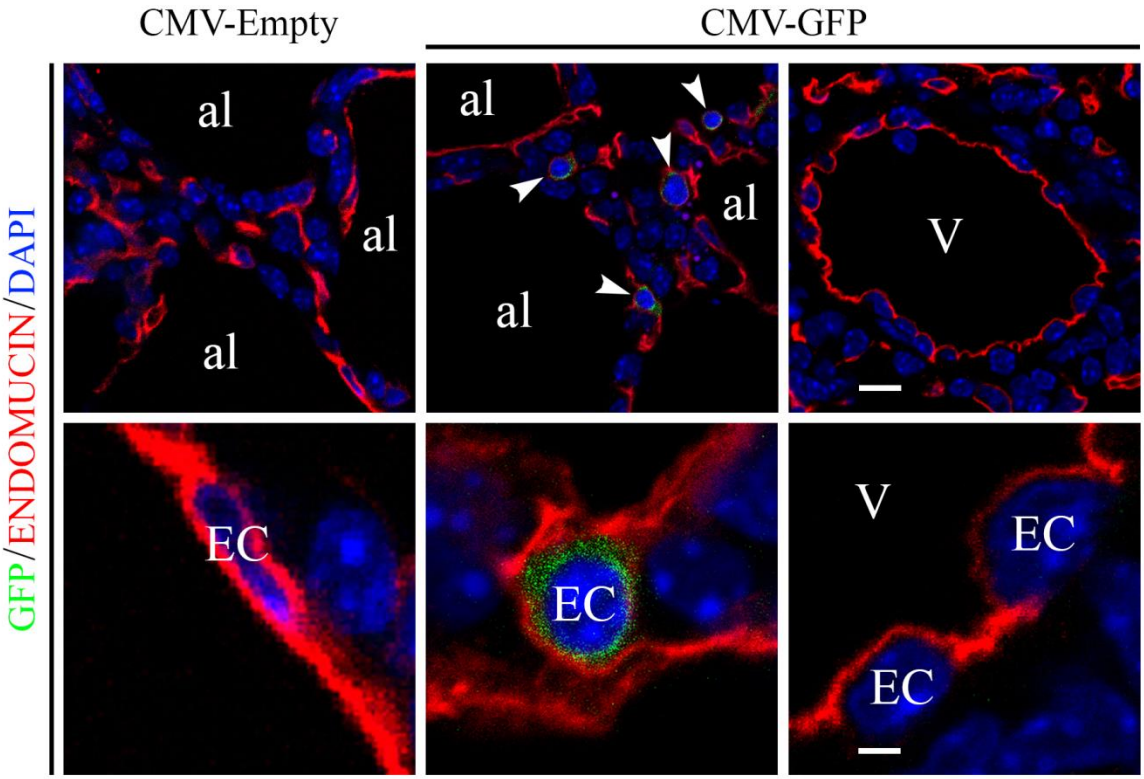
CMV-Empty
CMV-GFP
GFP/ENDOMUCIN/DAPI
al
al
al
al
al
V
EC
EC
V
EC
EC

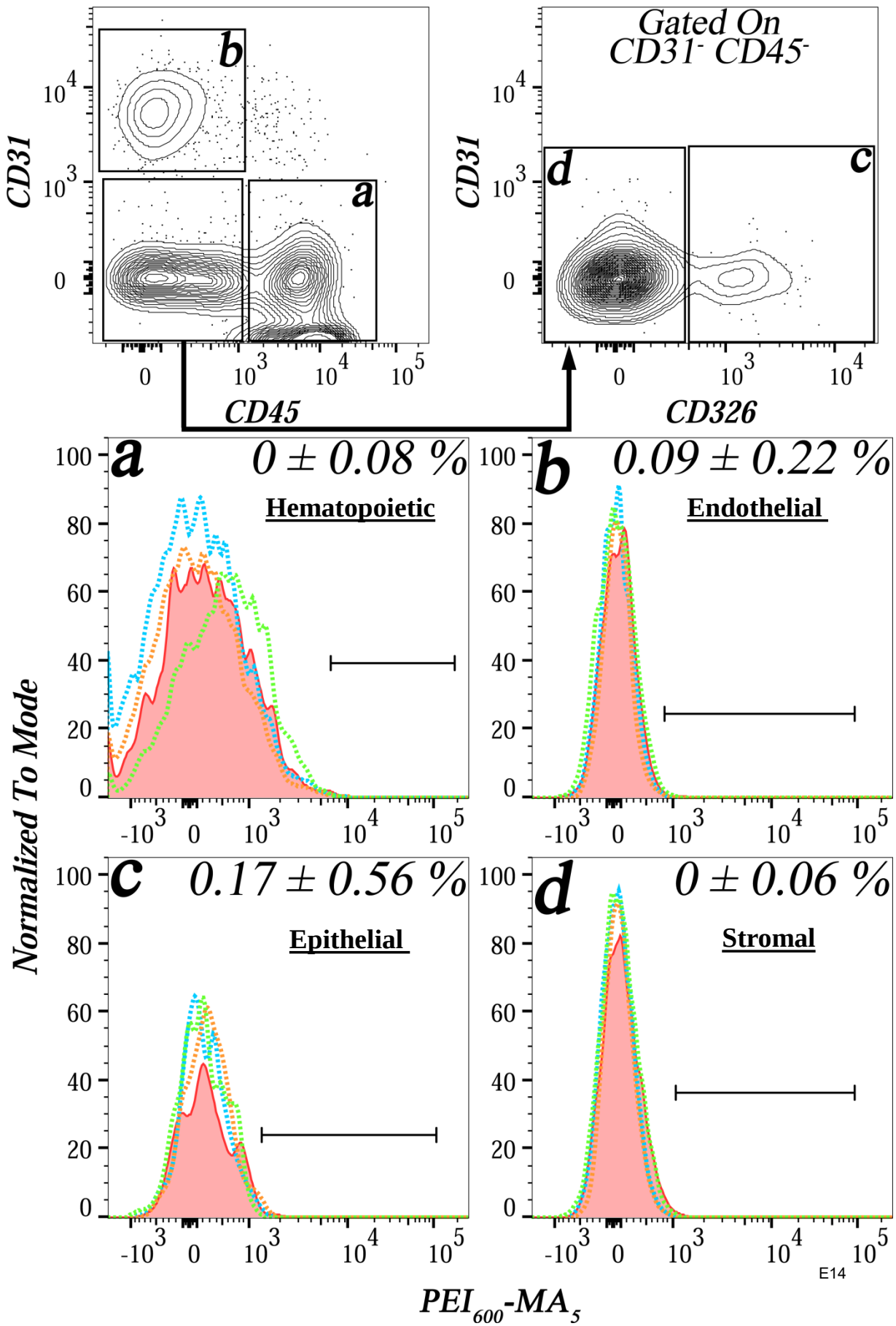
b
a
CD31
CD45
Gated On
CD31- CD45-
d
c
CD326
a
0 ± 0.08 %
Hematopoietic
b
0.09 ± 0.22 %
Endothelial
c
0.17 ± 0.56 %
Epithelial
d
0 ± 0.06 %
Stromal
Normalized To Mode
PEI600-MA5
E14

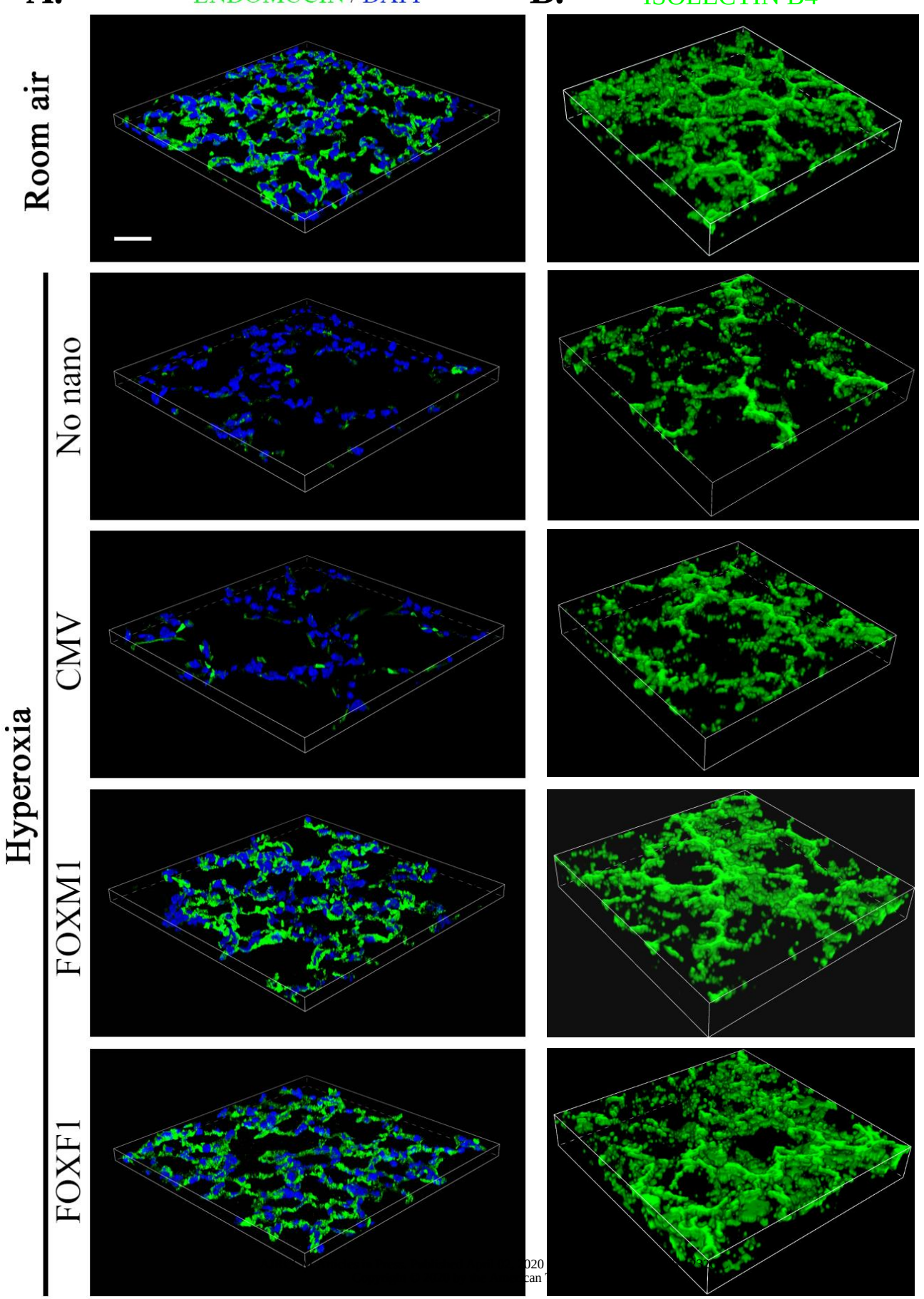
A.
ENDOMUCIN / DAPI
B.
ISOLECTIN B4
Room air
Hyperoxia
No nano
CMV
FOXM1
FOXF1

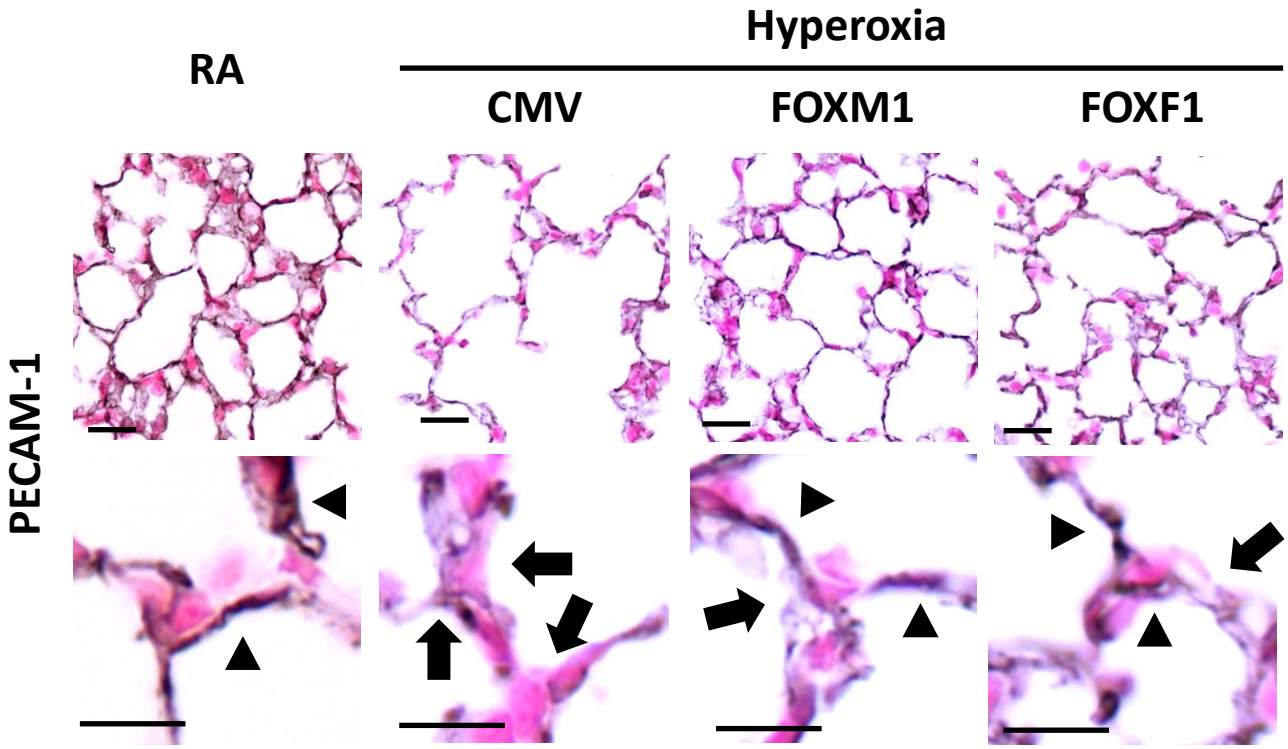
RA
Hyperoxia
CMV
FOXM1
FOXF1
PECAM-1

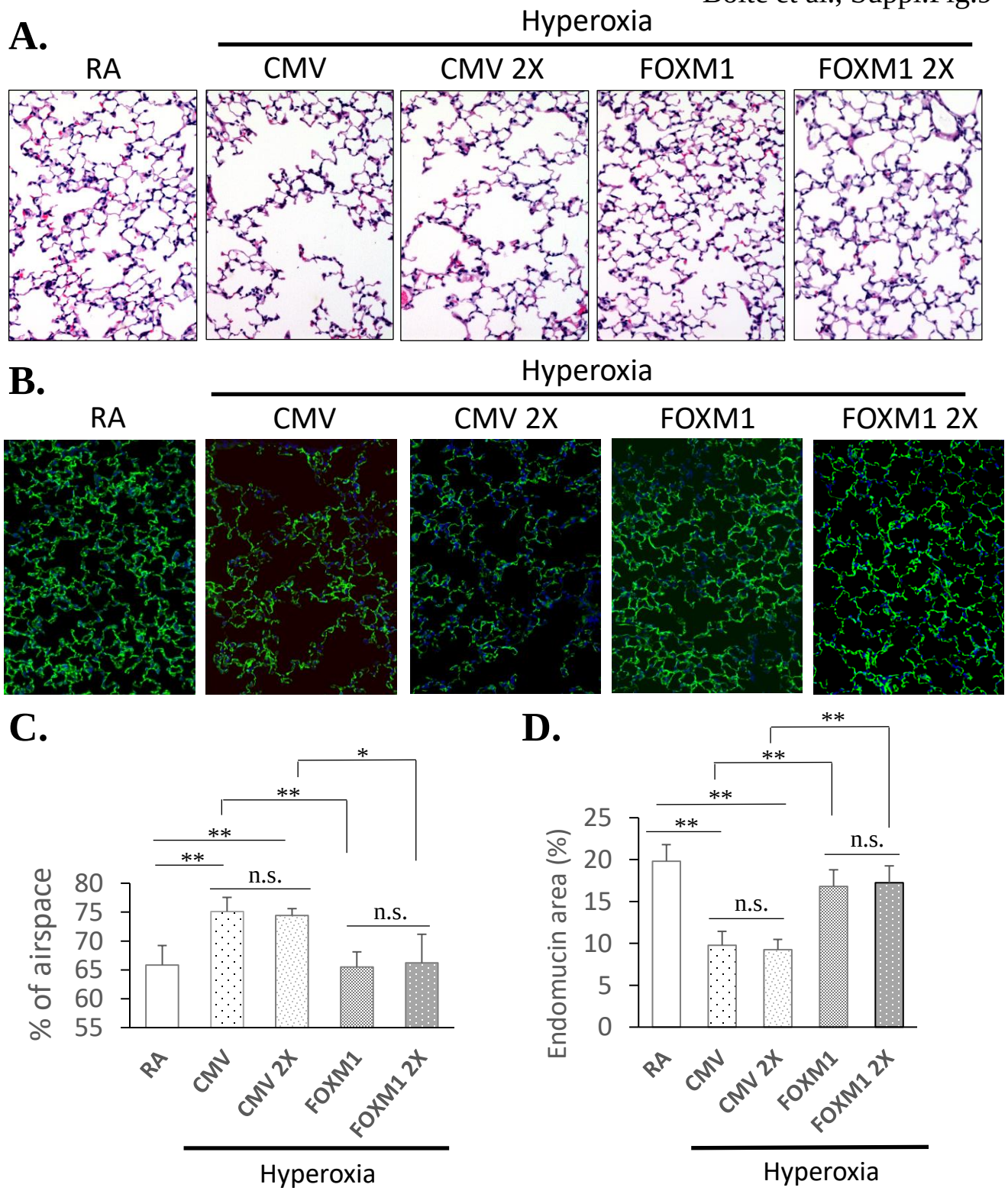
A.
Hyperoxia
RA
CMV
CMV 2X
FOXM1
FOXM1 2X
B.
Hyperoxia
RA
CMV
CMV 2X
FOXM1
FOXM1 2X
C.
% of airspace
80
75
70
65
60
55
*
**
**
**
n.s.
n.s.
RA
CMV
CMV 2X
FOXM1
FOXM1 2X
Hyperoxia
D.
Endomucin area (%)
25
20
15
10
5
0
**
**
**
**
n.s.
n.s.
RA
CMV
CMV 2X
FOXM1
FOXM1 2X
Hyperoxia

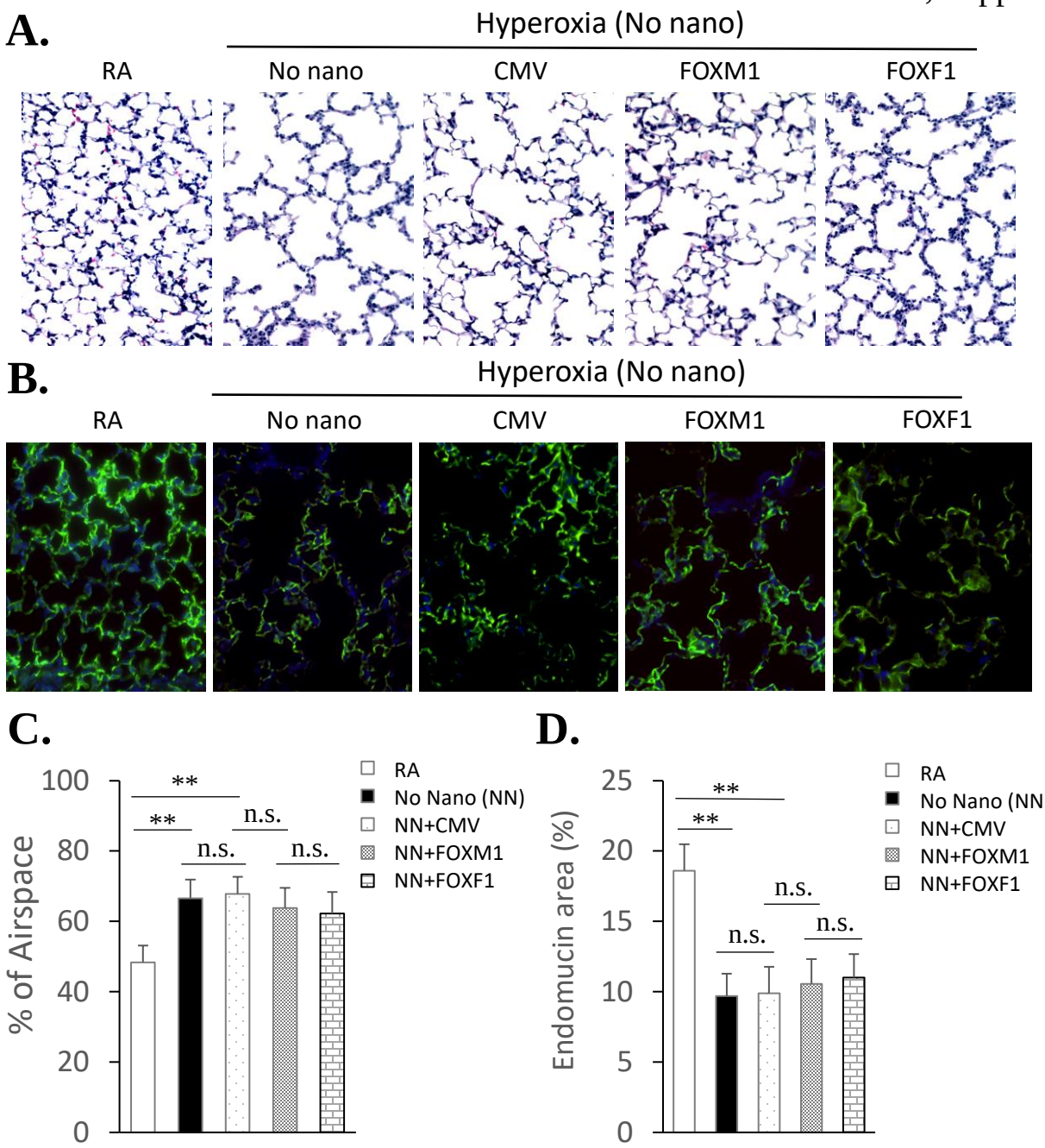
A.
Hyperoxia (No nano)
RA
No nano
CMV
FOXM1
FOXF1
B.
Hyperoxia (No nano)
RA
No nano
CMV
FOXM1
FOXF1
C.
% of Airspace
100
80
60
40
20
0
**
**
n.s.
n.s.
n.s.
RA
No Nano (NN)
NN+CMV
NN+FOXM1
NN+FOXF1
D.
Endomucin area (%)
25
20
15
10
5
0
**
**
n.s.
n.s.
n.s.
RA
No Nano (NN)
NN+CMV
NN+FOXM1
NN+FOXF1

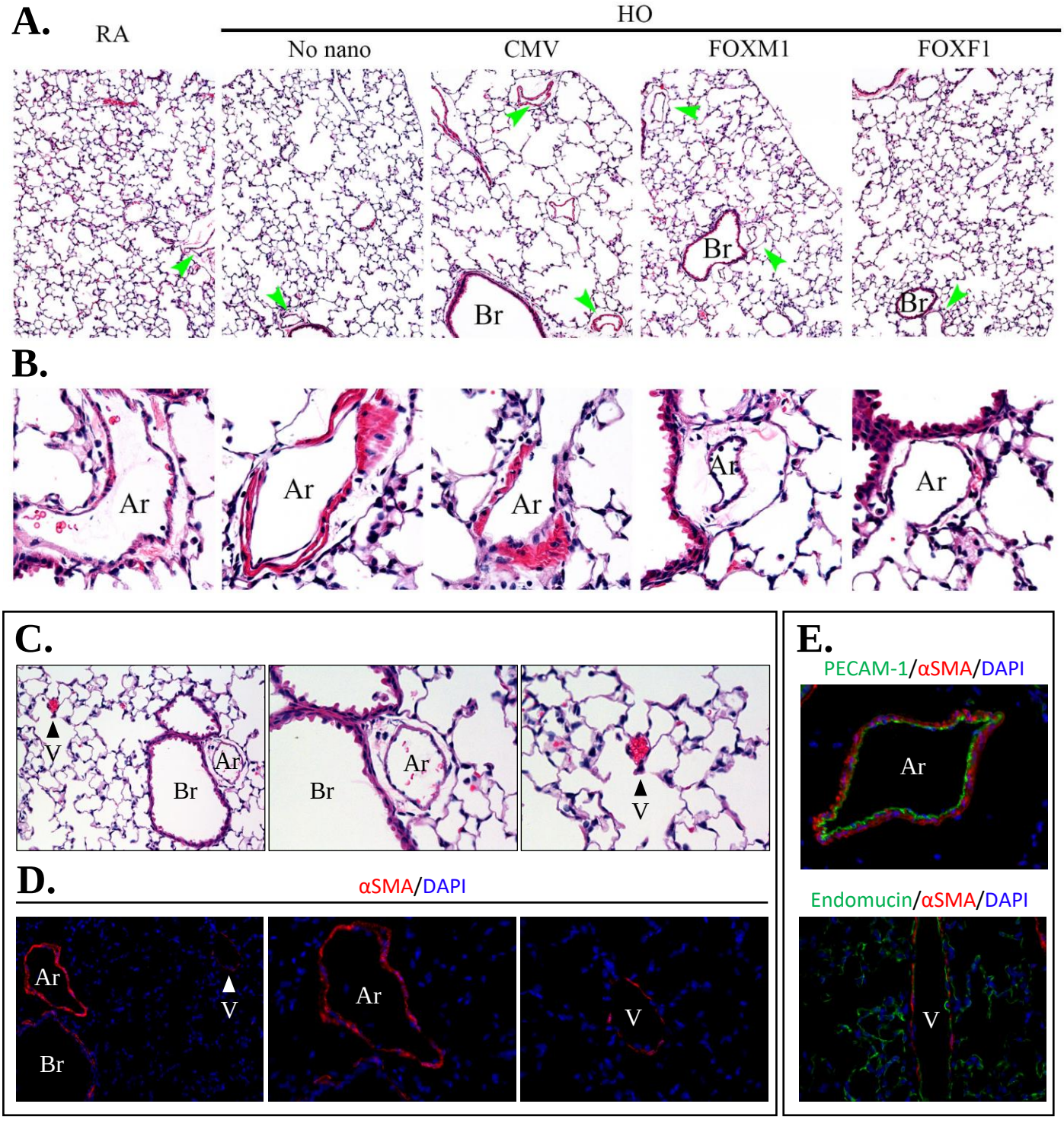
A.
RA
HO
No nano
CMV
FOXM1
FOXF1
Br
Br
Br
B.
Ar
Ar
Ar
Ar
Ar
C.
V
Ar
Br
Br
Ar
V
D.
αSMA/DAPI
Ar
V
Br
Ar
V
E.
PECAM-1/αSMA/DAPI
Ar
Endomucin/αSMA/DAPI
V

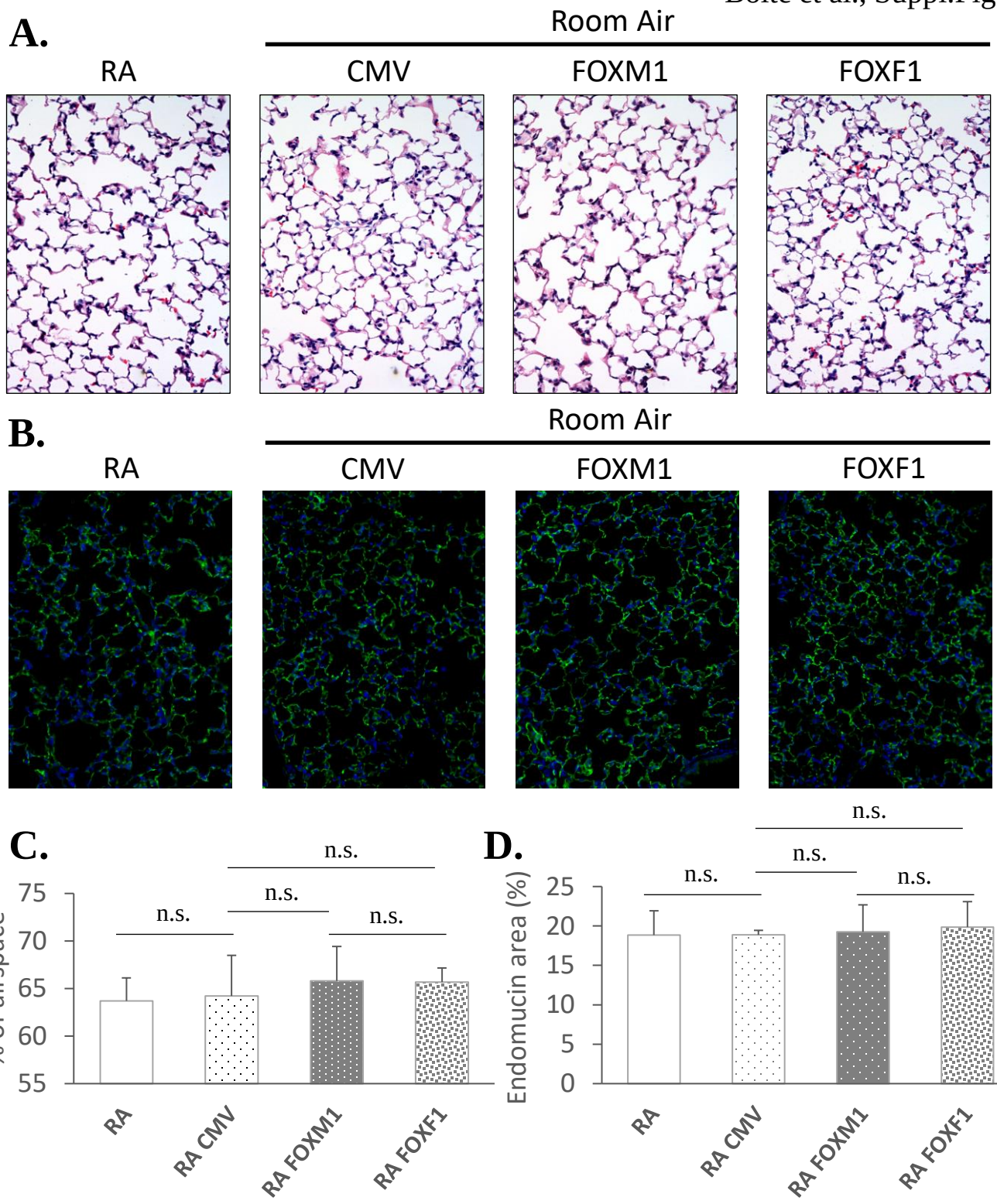
A.
Room Air
RA
CMV
FOXM1
FOXF1
B.
Room Air
RA
CMV
FOXM1
FOXF1
C.
% of airspace
75
70
65
60
55
n.s.
n.s.
n.s.
RA
RA CMV
RA FOXM1
RA FOXF1
D.
Endomucin area (%)
25
20
15
10
5
0
n.s.
n.s.
n.s.
RA
RA CMV
RA FOXM1
RA FOXF1

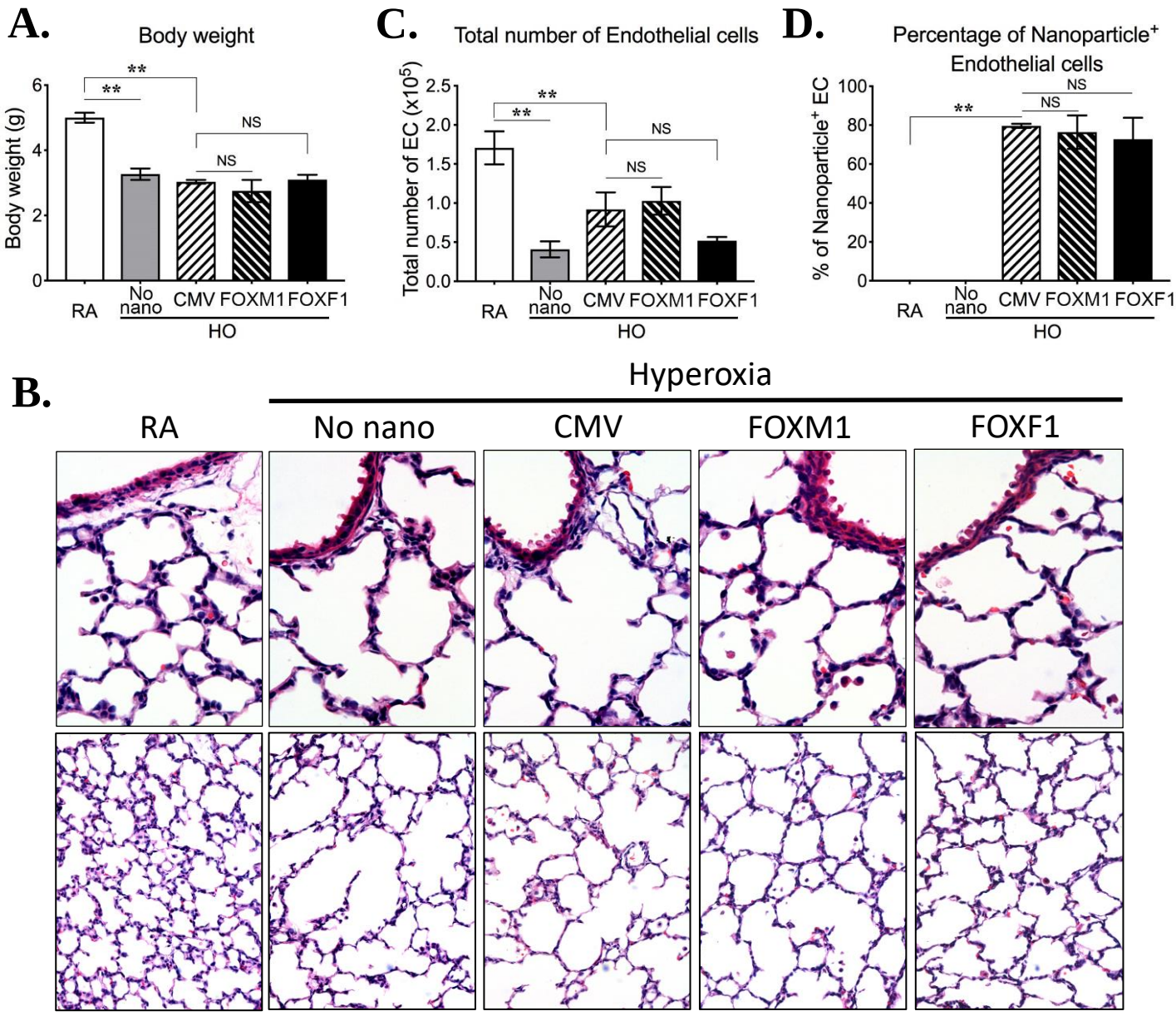
A.
Body weight
Body weight (g)
RA
No nano
CMV
FOXM1
FOXF1
HO
**
**
NS
NS
C.
Total number of Endothelial cells
Total number of EC (x10^5)
D.
Percentage of Nanoparticle+ Endothelial cells
% of Nanoparticle+ EC
B.
Hyperoxia
RA
No nano
CMV
FOXM1
FOXF1

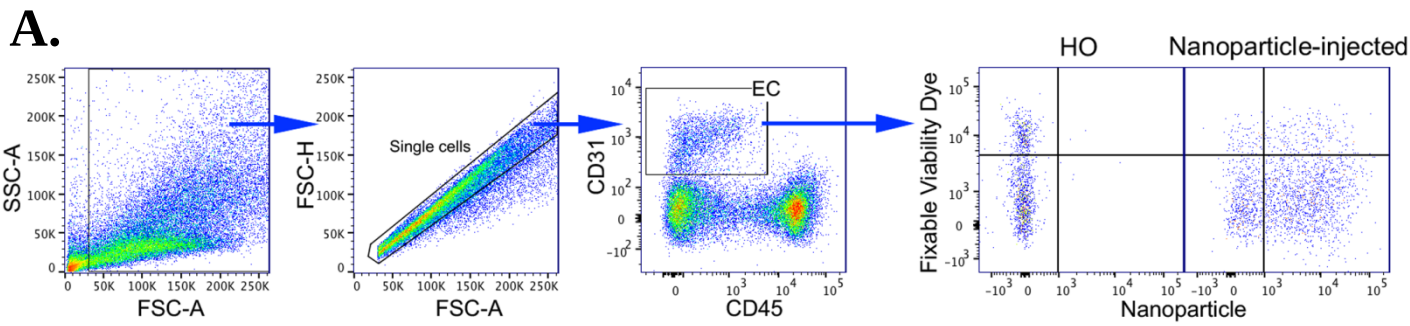
A.
SSC-A
FSC-A
FSC-H
Single cells
CD31
EC
CD45
HO
Nanoparticle-injected
Fixable Viability Dye
Nanoparticle

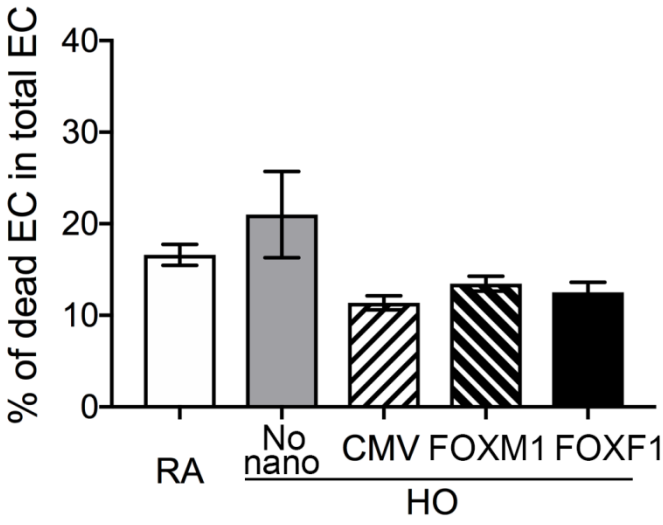
B.
% of dead EC in total EC
RA
No nano
CMV
FOXM1
FOXF1
HO

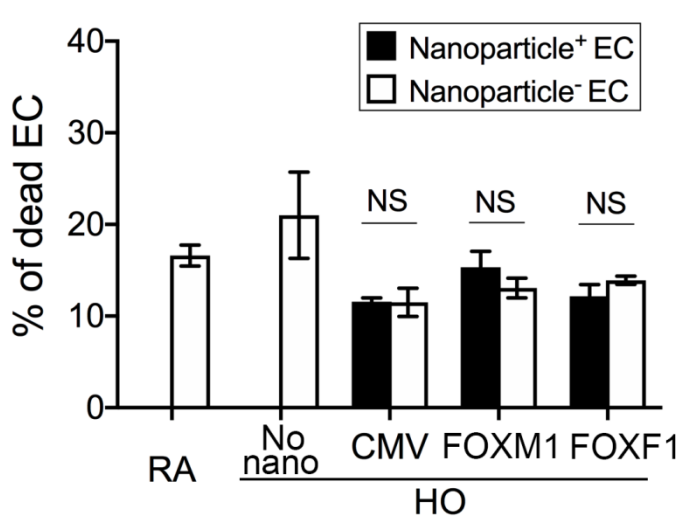
C.
% of dead EC
Nanoparticle+ EC
Nanoparticle- EC
NS
NS
NS
RA
No nano
CMV
FOXM1
FOXF1
HO

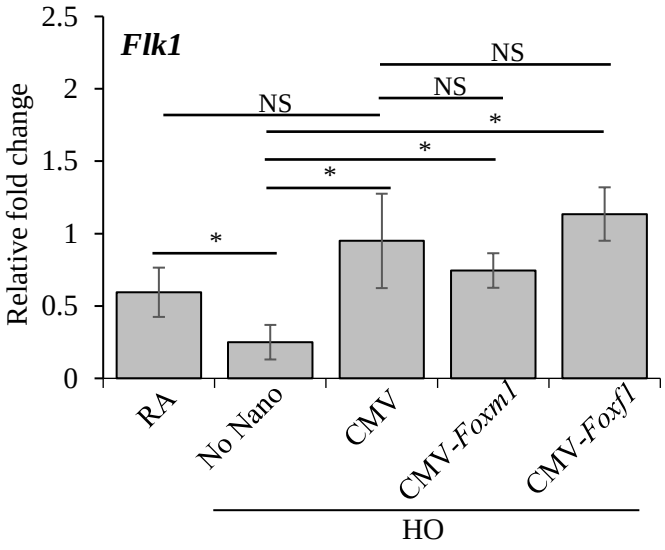
Flk1
Relative fold change
2.5
2
1.5
1
0.5
0
NS
NS
NS
*
*
*
*
RA
No Nano
CMV
CMV-Foxm1
CMV-Foxf1
HO

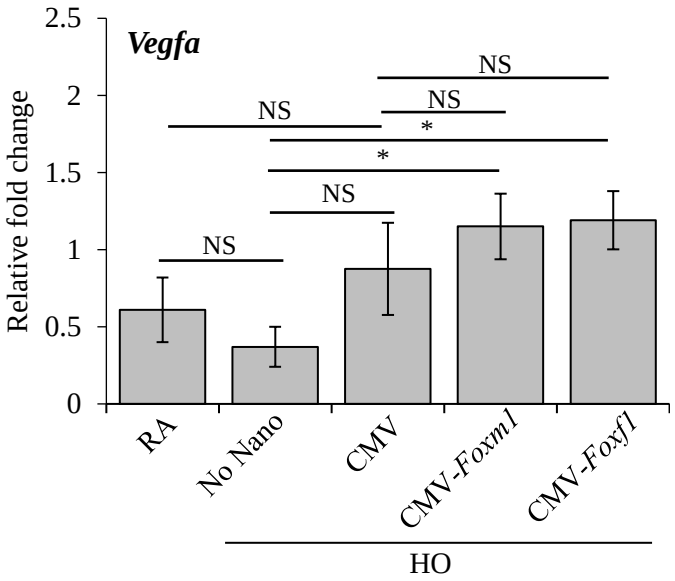
Vegfa
Relative fold change
2.5
2
1.5
1
0.5
0
NS
NS
NS
NS
*
*
NS
RA
No Nano
CMV
CMV-Foxm1
CMV-Foxf1
HO

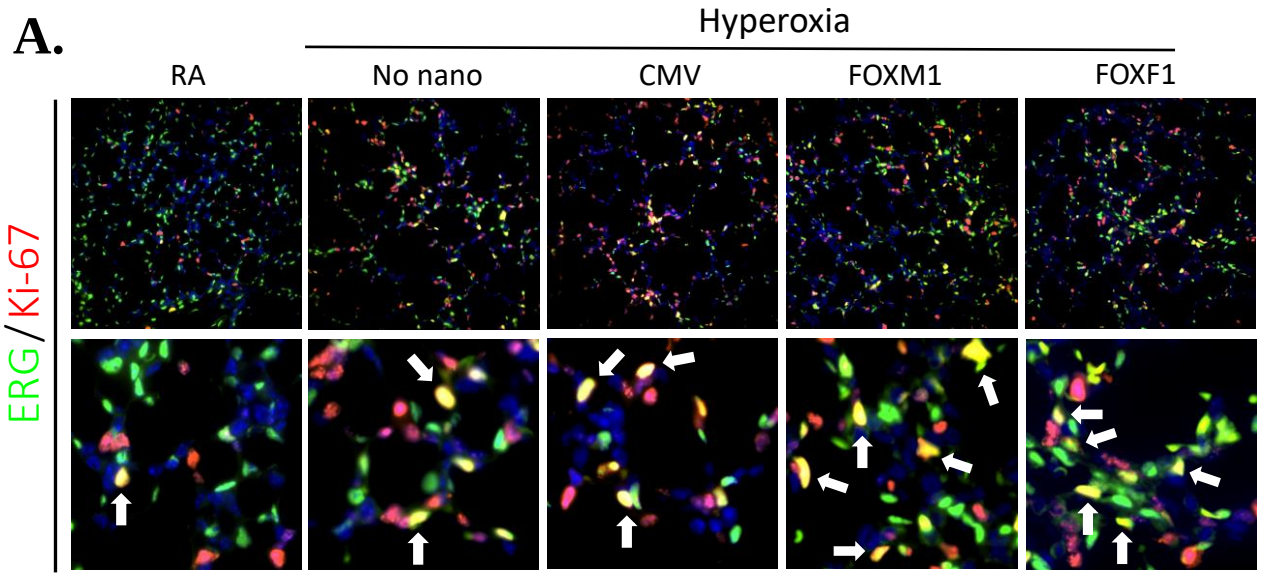
A.
Hyperoxia
RA
No nano
CMV
FOXM1
FOXF1
ERG / Ki-67

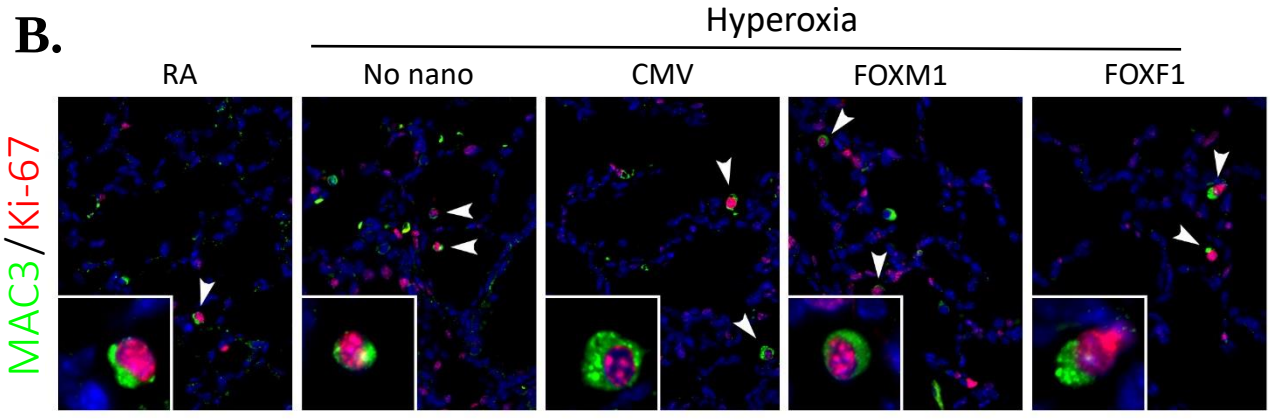
B.
Hyperoxia
RA
No nano
CMV
FOXM1
FOXF1
MAC3 / Ki-67

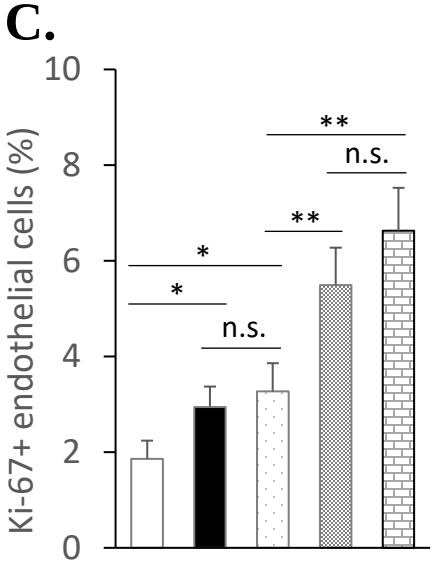
C.
Ki-67+ endothelial cells (%)
10
8
6
4
2
0
*
*
n.s.
**
**
n.s.
RA
HO alone
HO+CMV
HO+FOXM1
HO+FOXF1

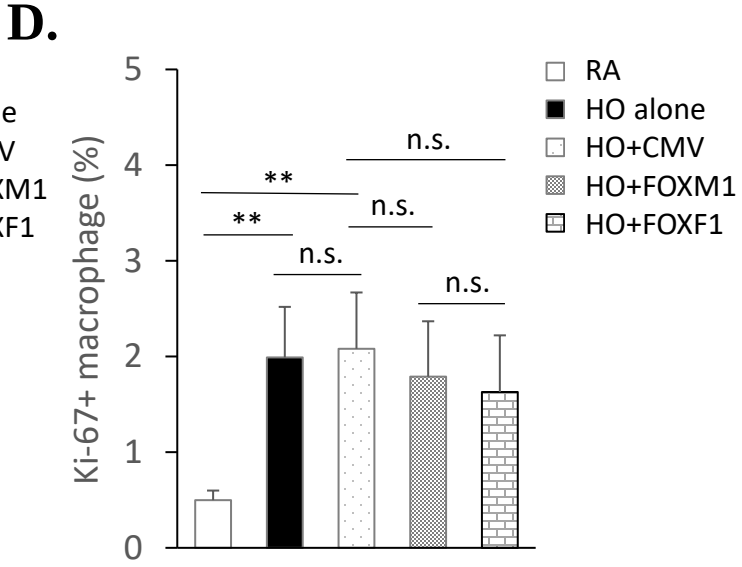
D.
Ki-67+ macrophage (%)
5
4
3
2
1
0
**
**
n.s.
n.s.
n.s.
n.s.
RA
HO alone
HO+CMV
HO+FOXM1
HO+FOXF1